Inorganic Chemistry

Article

pubs.acs.org/IC

Characterization of a Photoswitching Chelator with Light-Modulated Geometric, Electronic, and Metal-Binding Properties

Andrew T. Franks,[†] Degao Peng,[†] Weitao Yang,[†,‡] and Katherine J. Franz*[,†]

[†]Department of Chemistry, and [‡]Department of Physics, Duke University, Durham, North Carolina 27708, United States

Supporting Information

ABSTRACT: Photoswitching molecules are utilized for a variety of applications where the rapid manipulation of the molecules' chemical properties and spatial orientations allows for new spatiotemporal control over molecular-scale interactions and processes. Here, we present a hydrazone-containing transition metal chelator, HAPI ((*E*)-*N*′-[1-(2-hydroxyphenyl)ethyliden]isonicotinoylhydrazide), that displays dual-wavelength photoswitching behavior. Several of its metal complexes, however, are inert to photoreaction and thereby add another layer of control over the photoswitch system. The light-induced twist in HAPI structure is accompanied by a dramatic change in electronic properties as well as chelator strength. This work introduces HAPI as the prototype for a class of molecules with properties that may be optimized for a variety of experimental applications that take advantage of phototriggered molecular changes.

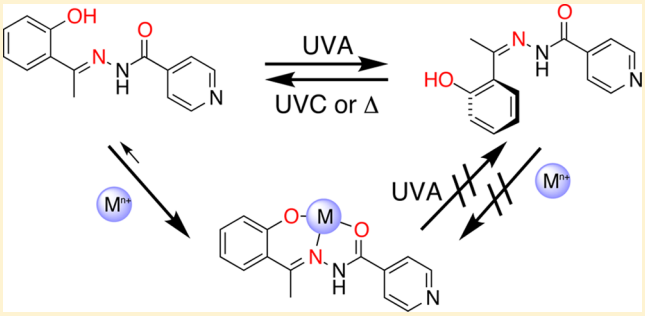

INTRODUCTION

Since azobenzene was first recognized as a photoswitching species in 1937 by Hartley,[1,2] it has become a workhorse for investigators wanting to control molecular arrangements with light.[3−13] The photoswitch toolbox has expanded beyond azobenzene in the past several decades, along with a growing number of multidisciplinary applications.[14−19] Tethering azobenzene derivatives or other photochromic moieties to biomolecules has enabled control over biological processes[20,21] such as ion release[22,23] and receptor activity,[24−26] while other work has focused on building light-driven molecular machines.[27,28]

In efforts to develop light-activated metal sensors and molecular logic gates, many photochromic scaffolds have been functionalized with metal-binding moieties.[14,29,30] These compounds are designed such that only one of the photoisomers presents an optimal metal binding site. In this way, azobenzenes outfitted with crown ethers can bind metal ions in solution only while in the photogenerated cis configuration; the ions are then released upon irradiation with visible light, which regenerates the weakly binding trans isomer (Figure 1a).[31,32] Metal chelating constructs have been cleverly introduced into other photochromic scaffolds, including spiropyrans[33−35] and spirooxazines,[36] which exhibit colorimetric or fluorometric changes in response to both metal binding and photoswitching (Figure 1b).

Analogous to azobenzenes, arylhydrazones are known to undergo photoinduced *E*/*Z* isomerization.[39] Recent studies from Lehn et al. have sought to utilize this reactivity for molecular logic systems[38] (Figure 1c) and stimulus-responsive chemistry from crystalline solids.[40] Schiff bases in general, and hydrazones in particular, favor the *E* isomer in their resting state.[41−47] The ability to accumulate the *Z* form depends on the presence of stabilizing intramolecular hydrogen bonds in the photogenerated state.[38,48,49] In these cases, light has only been shown to trigger *E*-to-*Z* isomerization, and other inputs like heat or acid are required to overcome the added stability and restore the initial *E* configuration.[50−52] One notable exception is the dual-wavelength switching behavior reported by Pichon et al.[53] Such reversible photoswitching activity, where different wavelengths of light can be used to toggle between two configurations, is highly desirable for some phototriggered applications.

In addition to light, triggers like a change in pH or the presence of a metal ion have also been used as the impetus for *E*/*Z* switching in some hydrazones.[48,54−57] In the case of the metal-controlled isomerization, multidentate coordination of a Zn^{2+} ion induces isomerization, and reversibility is achieved by addition of a competitive metal chelator.[56,57] It is notable that in all observed cases, hydrazone switching has been reported exclusively in organic solvent, presumably a requirement to maintain the *Z*-stabilizing interactions over extended periods of time.

A metal chelating subset of aroylhydrazones, exemplified by pyridoxal isonicotinoyl hydrazone (PIH) and salicylaldehyde isonicotinoyl hydrazone (SIH), has been investigated in cell culture and animal models for potential application in treating pathological iron misregulation.[58−63] The relative lipophilicity of these compounds as well as their high affinity for iron

Received: August 30, 2013
Published: January 15, 2014

   dx.doi.org/10.1021/ic402221x | *Inorg. Chem.* 2014, 53, 1397−1405

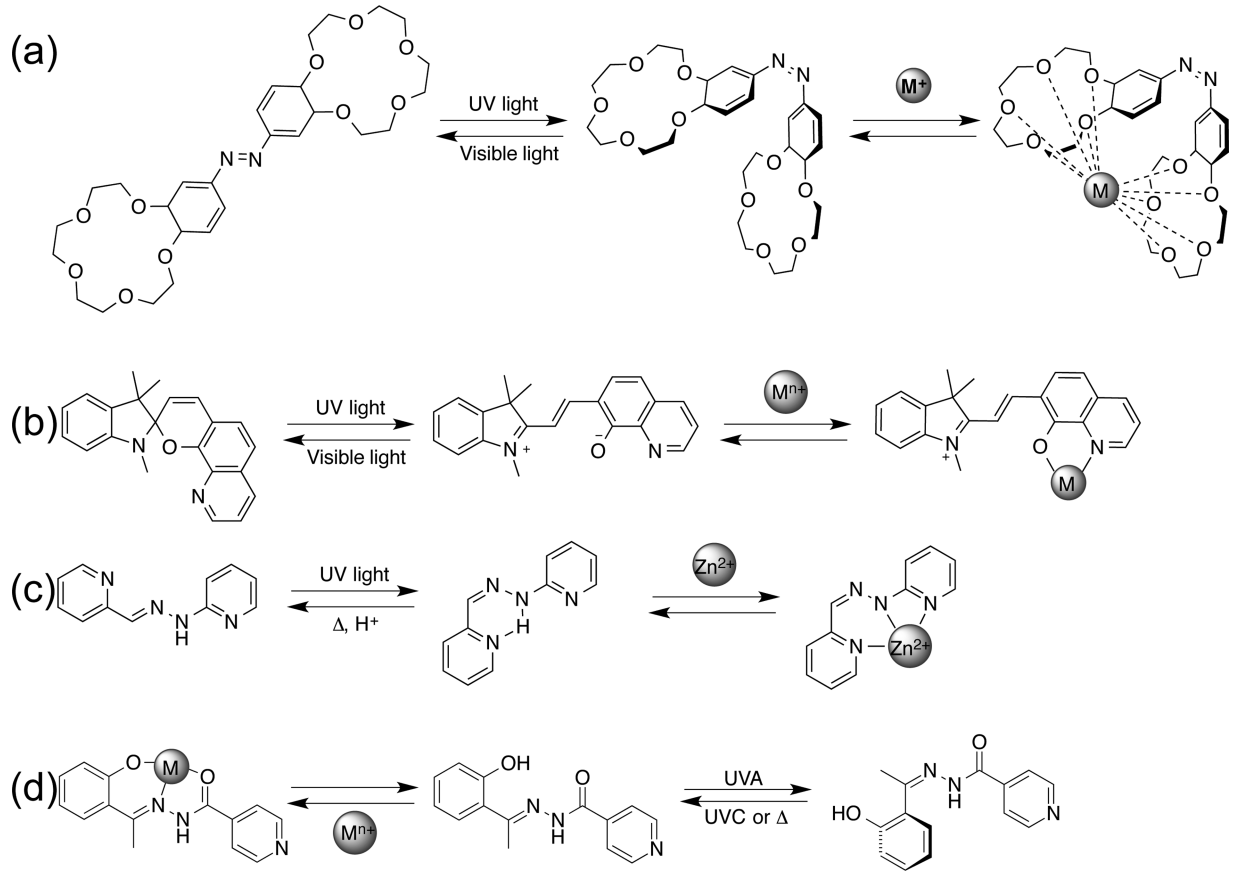

Figure 1. Examples of light switchable metal chelators built on three classes of photochromic molecules: (a) azobenzene, (b) spiropyran, and (c and d) hydrazone. (a) Azobenzene with incorporated crown ether moieties are brought into closer proximity by photoactivated trans−cis isomerization, effectively binding alkali metals.[31,32] (b) A spiropyran derivative of 8-quinolinol is nonbinding in its ring-closed form. UV-induced ring-opening exposes a phenolate O and creates a site for bidentate chelation of Zn^{2+}, Cu^{2+}, or Fe^{3+}.[34,37] (c) Light-triggered isomerization of the stable *E* arylhydrazone generates a stabilized *Z* isomer that is preorganized to bind Zn^{2+}.[38] (d) This work: HAPI binds transition metals in its stable *E* isomer, but photoisomerizes to a *Z* configuration with reduced metal affinity. Stable (*E*)-HAPI metal complexes are unreactive to photoisomerization.

confers improved biological activity over many canonical chelation therapeutics.[64] Aroylhydrazones with *N*-[*o*-hydroxyphenyl] moieties, such as PIH or HAPI, may exist as several tautomeric forms in solution. On the basis of previous studies of the structurally similar PIH, the enolimine depicted in the present work is believed to be the dominant species in aqueous solution at pH 7.4.[65]

These ligands use their phenolate O, imine N, and carbonyl O donor atoms to form both 1:1 and 2:1 ligand:metal complexes.[66−68] For example, crystal structures show Cu^{2+} binds in a 1:1 ligand:Cu molar ratio,[69] whereas Fe^{3+} forms either 1:1[70,71] or 2:1[58,72] ligand:Fe complexes depending on the conditions.[73] Recent work from Simunek and co-workers uncovered an SIH-like hydrazone with improved stability in plasma, ((*E*)-*N*′-[1-(2-hydroxyphenyl)ethyliden]-isonicotinoylhydrazide) (HAPI).[59] The introduction of a methyl group at the azomethine carbon confers hydrolytic stability without altering the tridentate presentation of donor atoms characteristic of this class of chelating agent.

We present here a study of the metal-gated reversible photochemistry of HAPI (Figure 1d), first highlighted as a promising candidate for biological iron chelation.[59] Photoswitching of HAPI geometry modulates electronic conjugation as well as metal-binding efficiency in this small molecule chelator.

RESULTS AND DISCUSSION

HAPI/HAPI* Photoreactivity. The UV/visible absorption spectrum of HAPI in pH 7.4 buffer shows characteristic bands at 288, 325, and 400 nm. As shown in Figure 2a, UVA irradiation (wavelength range ∼400−315 nm) of the HAPI solution attenuates the two longer wavelength bands and induces a 13 nm hypsochromic shift of the 288 nm band. The inset in Figure 2a shows more clearly the accompanying isosbestic point at 280 nm, which signals the presence of two cleanly interconverting species in solution. Over the course of several hours in the dark, the original spectral features return (Figure 2b). Recording the changes at 400 and 325 nm over time revealed a half-life for the photoexcited species of 5.7 ± 0.3 h. These results suggest that photoexcitation of HAPI generates a metastable species, which we term HAPI*, that thermally relaxes back to HAPI. The loss of absorption between 300−450 nm upon irradiation of HAPI suggests a significant loss of electronic conjugation across the molecule, while the reversibility implies that such changes are not permanent. Similar photoinduced blue shifts in absorption with thermal reversibility have been observed previously for arylhydrazones and are consistent with *E*/*Z* isomerization about the hydrazone C═N bond.[38,44,53]

Consistent with the hypothesis that irradiation of HAPI converts it to a metastable isomer is the fact that two species with different elution profiles but identical masses are separable

dx.doi.org/10.1021/ic402221x | Inorg. Chem. 2014, 53, 1397−1405

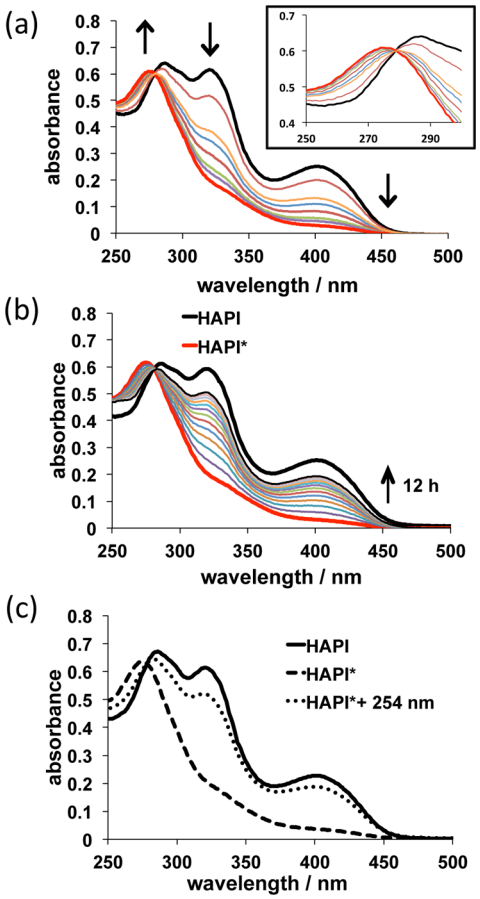

Figure 2. UV/vis absorption spectra demonstrating key features of HAPI reactivity. (a) The spectrum of HAPI (solid bold line, 50 μM HAPI in aqueous 10 mM HEPES buffer, pH 7.4, 200 mM NaCl) changes dramatically due to irradiation with UVA light (4 min total; spectra shown at 30 s intervals) to generate the red spectrum (HAPI*). The inset highlights the clean isosbestic point. (b) Left in the dark over 12 h, the irradiated solution of HAPI* shows the slow return of HAPI spectral features due to a thermal relaxation process. (c) Irradiation of a HAPI* solution (dashed line) for 1 min with UVC light centered at 254 nm restores the HAPI electronic spectrum (dotted line).

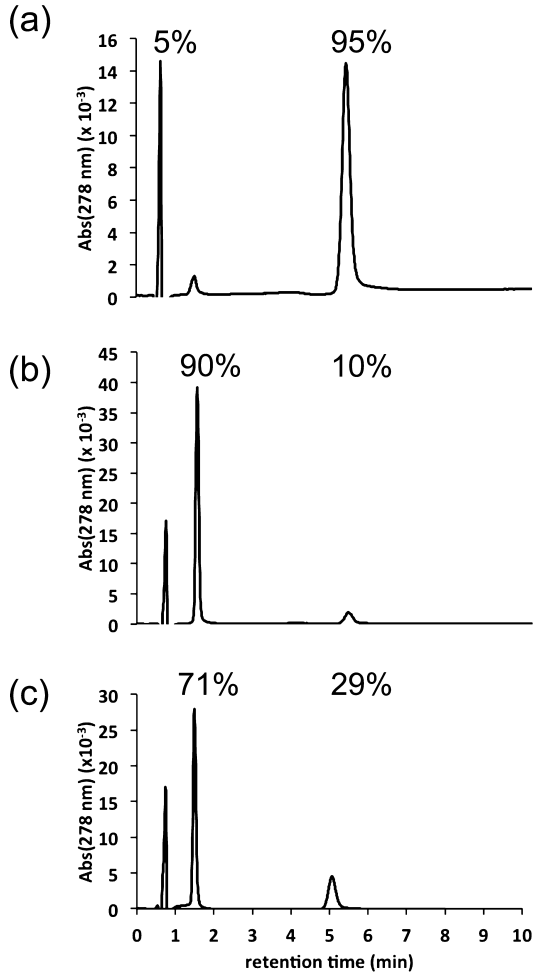

Figure 3. Chromatograms of solutions containing HAPI (a) before irradiation, (b) after 6 min of UVA irradiation, and (c) 3 h after the irradiated solution sat in the dark, showing the conversion of HAPI from its ground-state form to another distinct species, then returning toward the original abundances. Absorbance was measured at 278 nm where *E* and *Z* isomers share an isosbestic point (in 20% acetonitrile/80% H_2O, pH 7.4). The peak eluting at 5.3 min is (*E*)-HAPI and the 1.5 min peak is (*Z*)-HAPI, while the peak eluting before 1 min consists of solvent front buffer components.

by liquid chromatography. Chromatograms of nonirradiated HAPI solutions show one major peak eluting after 5.3 min, with a very minor peak eluting at 1.5 min under these chromatography conditions (Figure 3a). After 4 min of UV exposure, the ratio of these two peaks is inverted, with the bulk of the material eluting at the earlier time point (Figure 3b). Abundance of the photoproduct isomer in pre- and postirradiation solutions is found to be 4 ± 2% and 94 ± 4%, respectively. A chromatogram of the same irradiated sample collected 3 h after irradiation (Figure 3c) exhibits a partial reversion back to the original peak distribution. This re-equilibration is expected on the basis of the half-life of the photoproduct calculated from the UV−vis absorption data above. In-line mass spectrometry reveals *m*/*z* values of 256.1082 and 256.1099 for each peak, respectively, which matches the predicted exact mass for the $[M + H]^+$ ion for the HAPI molecule of formula $C_{14}H_{13}N_3O_2$. On the basis of these results, we assigned the later-eluting peak to the ground state *E* isomer and the earlier eluting peak to the metastable *Z* isomer.

^{1}H NMR spectroscopy was used to further probe the nature of the two distinct isomers. Spectra of HAPI collected in aprotic d_6-DMSO reveal signals for the amide (11.59 ppm) and phenolic (13.19 ppm) protons that would be expected to shift as a result of *E*/*Z* isomerization. The particularly deshielded phenolic proton peak in (*E*)-HAPI is indicative of a strong intramolecular hydrogen bond with the imine nitrogen, which is consistent with crystal structures for PIH, SIH, and other aroylhydrazones. In the current D_2O/DMSO mixture used for the photoisomerization studies, however, both proton signals are lost due to exchange with solvent and therefore cannot assist in the structural assignment of HAPI*. After 10 min of irradiation in D_2O/DMSO, the proton resonances nearest the C═N bond (H_d, H_e, and H_f) significantly shift upfield in the HAPI* spectrum as compared to that of HAPI (Supporting Information Figure S3). There are no observed changes in integrated peak area or splitting, suggesting that the light-driven process being observed is a spatial reorganization rather than a change in connectivity. It is also interesting to note that under the conditions used in this NMR experiment, no *Z* isomer is observed in the sample prior to irradiation. This result contrasts with the small concentrations of (*Z*)-HAPI observed in

dx.doi.org/10.1021/ic402221x | Inorg. Chem. 2014, 53, 1397−1405

preirradiated solutions by HPLC and LC−MS. It should be noted, however, that the solution conditions between these methods differ in pH, ionic strength, and temperature, as the NMR sample was dissolved in an unbuffered solution of D_2O and DMSO with no added salts and analyzed at 10 °C. From these results, we attribute the clear changes in chemical shifts between HAPI and HAPI* to a configurational change about the hydrazone bond.

To test for photoreversibility, solutions of HAPI* were further irradiated with low-pressure Hg lamps, which exhibit a strong emission band in the UVC (ultraviolet C radiation of wavelength range 280−100 nm) range at 254 nm. As shown in Figure 2c, such exposure results in rapid restoration of the original HAPI spectrum. This result was also confirmed by LC−MS (data not shown) and demonstrates that isomerization of HAPI can be toggled from *E* to *Z* by UVA light, and from *Z* back to *E* by UVC light. This is a rare example of a reversible chelating hydrazone system that uses different wavelengths of light, rather than chemical input, to trigger both "on" and "off" switching.

Theoretical Modeling. To gain structural insight that might explain the magnitude of changes observed experimentally, we performed geometry optimizations of the (*E*)-HAPI and (*Z*)-HAPI isomers using the B3LYP[74,75] functional and the polarizable continuum model (PCM) with Gaussian 09[76] (see the Supporting Information for calculation details). Calculation results reveal that in its expected *E* form, the molecule adopts a planar structure. This predicted structure is similar to the experimentally determined crystal structure of SIH and related aroylhydrazones.[66] If forced into a *Z* configuration, however, steric clashing between the phenol-bearing aromatic ring and the hydrazido proton results in rotation of the phenol out of the molecular plane (Figure 4), increasing the calculated

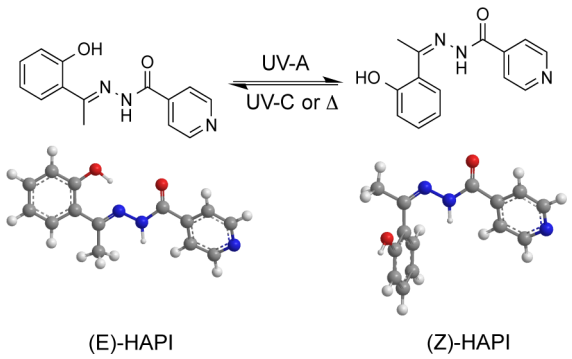

Figure 4. Exposure of (*E*)-HAPI to UVA light induces photoisomerization. The proposed structure for the metastable product, HAPI*, features the *Z* configuration about the hydrazone bond. In computer models, steric hindrance forces the phenol ring out of the plane of the molecule.

dihedral angle between the phenol ring and the hydrazone C═N bond from 3° to 76°. This dihedral twist disrupts the stabilizing π orbital overlap that extends the length of the molecule in the *E* configuration. Such a disruption in electronic character would be predicted to result in loss of features in the electronic absorption spectrum, which is indeed the experimental observation.

To gain more insight into these electronic states, we performed time-dependent density functional theory (TD-DFT) calculations for the *E* and *Z* configurations of HAPI. Indeed, the computational results predict transitions between electronic states that mirror the transitions observed experimentally by UV/visible absorption spectroscopy. The small offsets ranging from 10−30 nm between experimental and predicted absorption bands (Supporting Information Figure S1) are likely due to explicit solvent effects that are not accounted for in the computational model. Regardless of these offsets, the calculations predict a blue shift of about 50 nm for the lowest excitation energy of (*Z*)-HAPI as compared to (*E*)-HAPI. This prediction matches the difference in the lowest energy λ_{max} values experimentally observed at 275 and 325 nm for (*Z*)-HAPI and (*E*)-HAPI, respectively.

Computations also predict that the *E* configuration is 6.3 kcal/mol more stable than *Z*. The calculated result that the *Z* form is higher in energy is consistent with the observed lack of HAPI* stability in solution. However, the magnitude of the calculated energy difference is larger than would be predicted on the basis of the experimental observation of a 96:4 equilibrium *E*:*Z* ratio in samples analyzed by HPLC before irradiation, a result that corresponds to a ΔG of only 2 kcal/mol. This discrepancy likely arises from multiple sources. First, although B3LYP is the best exchange-correlation functional for general purposes, typical B3LYP calculations exhibit uncertainties on the order of a couple kcal/mol.[77] Additionally, the PCM model used here does not account for interactions of the explicit solvent and the substrate; this ignores the possible effect that hydrogen bonding between the solvent and the substrates could have on the isomers' relative stabilities. Finally, all calculations are based on fully protonated species, whereas the experiments are done at a pH at which some fraction of deprotonated forms coexist.

Metal Binding. Aroylhydrazones like HAPI contain tridentate binding sites that are preorganized for efficient chelation of several di- and trivalent metal ions.[66] Formation of stable metal complexes could in principle prevent photoisomerization, as observed previously for Zn^{2+}-binding hydrazones.[38] To test this hypothesis, we irradiated buffered solutions of HAPI in the presence of a panel of metal ions. Addition of equimolar Al^{3+}, Fe^{3+}, Cu^{2+}, and Ni^{2+} all induce spectral changes indicative of metal−HAPI complex formation (Figure 5 and Supporting Information Figure S4). The new

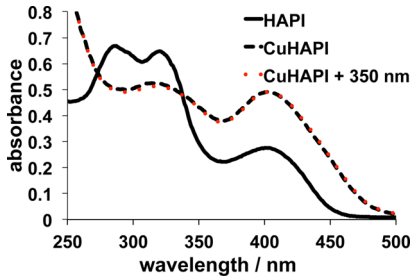

Figure 5. Treatment of 50 μM HAPI (black solid line) in 10 mM HEPES (pH 7.4, 200 mM NaCl) with 1 mol equiv of $CuSO_4$ generates a complex (black dashed) that does not change spectroscopically in response to 5 min irradiation with UVA light (red dotted).

spectra, however, do not change further upon UVA irradiation, suggesting that the hydrazone remains locked in its optimal *E* metal-binding configuration. Equimolar Mn^{2+}, Co^{2+}, and Zn^{2+} do not inhibit HAPI photoizomerization, although higher concentrations either block it (Mn^{2+} and Co^{2+}) or induce precipitation (Zn^{2+}), suggesting these metal ions bind HAPI

dx.doi.org/10.1021/ic402221x | Inorg. Chem. 2014, 53, 1397−1405

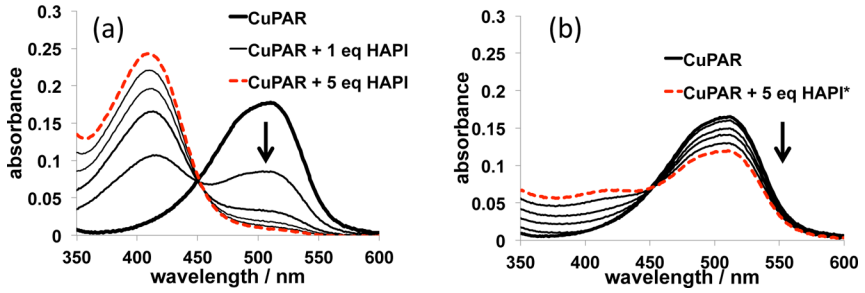

Figure 6. A 5 μM Cu(PAR) solution in PBS aqueous buffer was titrated with 1−5 mol equiv of either (a) HAPI or (b) photoirradiated HAPI (i.e., HAPI*). The absorption band at 510 nm is indicative of Cu(PAR) complex in solution. Absorption near 400 nm is attributable to both metal-free PAR and $[Cu(HAPI)]^+$. Addition of HAPI readily removes Cu^{2+} from PAR, whereas HAPI* chelation efficiency is reduced and removes far less copper at the same concentrations.

less tightly than those listed above (Supporting Information Figure S4). As expected, cations not expected to bind tightly to HAPI fail to inhibit the photoreaction, as evidenced by the spectral appearance of HAPI* even in the presence of 100-fold K^+, Ca^{2+}, or Mg^{2+} (Supporting Information Figure S4).

Metal-induced configurational "locking" was also probed by fluorescence, using the fluorescent probe calcein as a readout for potential Fe release from the HAPI complex (see Supporting Information Figure S9). In a solution containing calcein and preformed $[Fe(HAPI)_2]^+$ complex, Fe ions are sequestered by coordination to HAPI and the *apo* probe exhibits strong fluorescence. If metal-bound HAPI were to undergo photoisomerization, irradiating the complex should reduce the affinity of HAPI for Fe and result in the formation of a fluorescence-quenched Fe(calcein) complex. However, when $[Fe(HAPI)_2]^+$ is irradiated immediately prior to mixing with calcein, there is no difference in calcein emission, supporting the conclusion that stable coordination complexes formed by HAPI are inert to photoreaction.

Conditional binding constants for HAPI complexes with Zn^{2+}, Fe^{3+}, and Cu^{2+} were determined experimentally by competitive binding assays with Zincon, EDTA, and PAR, respectively, as explained in detail in the Experimental Section and shown in Supporting Information Figures S5−S8. The concentrations of all species in solution were determined by UV/visible absorbance spectroscopy. Through a global fit analysis, the constants were determined using the most appropriate ligand:metal binding model. These conditional constants are: $\log K'_{Zn(HAPI)} = 3.6 \pm 0.1$; $\log K'_{Cu(HAPI)} = 14.7 \pm 0.1$; and $\log K'_{Fe(HAPI)2} = 20.5 \pm 0.2$. The experimentally determined values establish that HAPI binds zinc with low affinity, while ferric and cupric ions are tightly complexed. These values reflect the complexation behavior observed spectroscopically for HAPI, and affirm the conclusion that HAPI remains configurationally locked while bound to metals in highly stable complexes. The relatively low affinity of HAPI for Zn^{2+} compared to Cu^{2+} and Fe^{3+} is consistent with previous assessments of metal affinity by phenol-bearing aroylhydrazone chelating agents.[78] Hydrazone ligands binding to Zn^{2+} are more likely to contain a pyridyl moiety instead of a phenol for metal chelation.[38,79−81] Those phenol-bearing ligands showing moderate or high affinity for Zn^{2+} have generally been studied at high pH or in primarily organic solvent.[82,83]

The metal-binding studies strongly suggest that preformed and stable metal−HAPI complexes are inert to photoisomerization. If the complexes are not preformed, however, the geometry-optimized structure of (*Z*)-HAPI shown in Figure 4 predicts that it should have a significantly diminished ability to bind metals as compared to (*E*)-HAPI. We tested this hypothesis by comparing the ability of HAPI versus HAPI* to extract Cu^{2+} from PAR (4-(2-pyridylazo)resorcinol), a ligand that forms a colored complex with Cu^{2+}. One molar equivalent of HAPI causes the characteristic Cu−PAR band at 510 nm to decrease by one-half, while 5 equiv is sufficient to cause a complete transition from the Cu−PAR spectrum to that of Cu−HAPI, proving that HAPI easily elicits complete transfer of Cu^{2+} from PAR to HAPI (Figure 6a). In contrast, a 5-fold excess of HAPI* leaves 70% of the Cu(PAR) spectrum intact, demonstrating a significantly decreased affinity of HAPI* for Cu^{2+} as compared to native HAPI (Figure 6b).

The differential affinity of HAPI versus HAPI* was also assessed for Fe^{3+} by a competitive binding assay, in this case by using calcein. Aliquots of HAPI, HAPI*, and UVC-irradiated HAPI* were mixed with solutions containing preformed Fe(calcein), which has a quenched fluorescence emission as compared to free calcein. Metal transfer from calcein to a competitive ligand restores calcein emission. As shown in Figure 7, HAPI itself readily restores calcein emission,

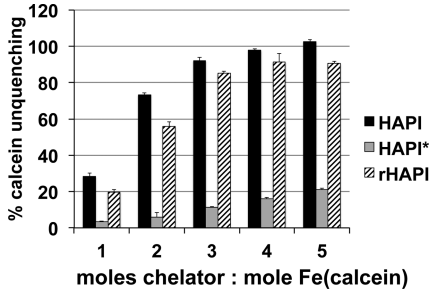

Figure 7. Relative iron binding strengths of HAPI, HAPI*, and UVC-reconstituted HAPI (rHAPI) as assessed by their ability to remove Fe^{3+} from calcein and thereby unquench calcein fluorescence. Readings were collected 10 min after mixing.

suggesting it strongly binds Fe^{3+}. In contrast, HAPI* has little effect on calcein quenching, consistent with it having a reduced affinity for Fe^{3+}. The affinity of HAPI* can be restored, however, by UVC irradiation, which returns HAPI* back to HAPI (referred to as rHAPI in Figure 7). The difference in calcein unquenching between HAPI and HAPI* shown in Figure 7 diminishes over the course of several hours, consistent with the thermal relaxation of HAPI* back HAPI (Supporting Information Figure S10).

dx.doi.org/10.1021/ic402221x | *Inorg. Chem.* 2014, 53, 1397−1405

CONCLUSIONS

We have identified in HAPI a dual-wavelength system for light-induced modification and restoration of molecular shape, electronic conjugation, and transition metal chelation efficacy. This hydrazone-containing transition metal chelator undergoes a photoinduced *E*-to-*Z* configurational switch about the hydrazone double bond that is observable by ^{1}H NMR spectroscopy, liquid chromatography, and UV/vis absorption spectroscopy. Conditional metal binding constants of HAPI determined for three first-row d-block metals agree with the observation that strongly binding metal ions, notably Fe^{3+} and Cu^{2+}, stabilize the *E* configuration such that the photoreaction does not proceed. In the absence of these metal ions, the loss of UV/vis spectral features upon photolysis indicates a light-induced break in the extended conjugation across the HAPI scaffold. Computational modeling of the *Z* isomer shows the phenol-bearing aromatic ring twists out of planarity with the rest of the molecule, providing a geometric rationale for the break in conjugation.

It is possible that many already synthesized compounds exhibit analogous chemistry, and a confluence of factors has led to these properties being overlooked. The increased steric bulk near the azomethine carbon in HAPI over that of aldehyde-based hydrazones (such as PIH and SIH) may both extend the lifetime of the metastable species as well as help enforce the dramatic structural change that accompanies the change in electronic absorption. At present, the mechanisms at work in the HAPI photoreactions (both UVA and UVC-induced) as well as the thermal relaxation of the *Z* isomer are not well understood, and it is unclear what unique aspect of the HAPI structure enables photoreversibility. A consequence of the blue shift in electronic absorption upon exposure to UVA light may be that preferential absorption of short-wavelength UVC irradiation by the *Z* isomer favors its excitation and subsequent photochemistry. The questions surrounding hydrazone photochemical and thermal isomerization are numerous and warrant further investigation.

For many applications, reversibility is a desirable feature for a photoswitching scaffold. That is, different wavelengths or intensities of light should be able to trigger both forward and reverse reactions in the switch. The on/off/on toggling of HAPI with light eliminates the need to wait for thermal relaxation or to add chemical modifiers, expanding the temporal control of this system beyond current photoactive hydrazones. The metal-dependent blocking of photoreactivity adds another layer of control over this system's reactivity, and the ability to generate large excesses of metastable photoproduct with even a modest lifetime in aqueous solution may enable new experimental designs. Furthermore, structures built on a HAPI scaffold could take advantage of the photoinduced molecular twist to alter electronic conjugation as well as induce 2D-to-3D structural changes.

Taking cues from azobenzene literature, modifications of the compound's structure will lead future efforts to tune thermal relaxation kinetics and the wavelengths needed for photoswitching. Control over these properties will lead to a more robust chemical tool for a variety of desired applications.

EXPERIMENTAL SECTION

General Notes. HAPI was synthesized as a crystalline solid according to published procedures.[59,84] All HAPI working solutions were prepared from a 10.1 mM stock solution in 100% DMSO. Phosphate-buffered saline (PBS, pH 7.4, 6.66 mM phosphate + 154 mM NaCl) solution was purchased from Lonza Corp. Solutions prepared with 2-[4-(2-hydroxyethyl)piperazin-1-yl]ethanesulfonic acid (HEPES) buffer were made with 10 mM HEPES (pH 7.4) and 200 mM NaCl unless otherwise noted. $CuSO_4$ stock solutions were standardized by titration with EDTA in pH 10 ammonia buffer to a murexide end point. For experiments using ferrous ammonium sulfate, $Fe(NH_4)_2(SO_4)_2$, solutions were prepared and standardized daily by redox titration using potassium dichromate as a primary standard. The Fe(II) titrant was added to a $K_2Cr_2O_7$ solution (acidified with H_2SO_4) to a ferroin indicator end point (blue-green to red). Irradiation for photoreactions was performed in Rayonet RPR-100 photoreactors; all samples were contained in quartz cuvettes. The photoreactors were equipped with either 16 RPR-3500 lamps that emit UVA light centered at 350 nm or 16 35 W low-pressure Hg lamps (RPR-2537) without phosphor coating, which emit a primary band at 254 nm.

Liquid Chromatography/Mass Spectrometry. All samples analyzed by liquid chromatography were prepared at a concentration of 50 μM in PBS buffer. Irradiated samples were first exposed in quartz cuvettes for 5 min of UVA light immediately prior to chromatographic analysis. An Agilent 1200 Series system was used for liquid chromatography with in-line high-resolution mass spectrometry (LC−MS). An Agilent Zorbax C8 (50 × 2.0 mm) column was held at 40 °C during data collection, and mass spectra were acquired on an in-line Agilent 6224 TOF-MS (time-of-flight mass spectrometer). Samples were separated by isocratic elution (80% A/20% B where A is 5 mM ammonium acetate, pH 7.5, and B is 98% acetonitrile/2% H_2O with 5 mM ammonium acetate, pH 7.5). UV chromatograms were collected by photodiode array detector set to 278 nm, the isosbestic point for the two isomers under elution conditions. Peak areas were integrated using MassHunter software.

^{1}H NMR Spectroscopy. All spectra were acquired using a Varian 500 MHz spectrometer at 10 °C to minimize thermal relaxation of metastable HAPI*. Samples were prepared from a 10 mM HAPI stock solution in d_6-DMSO by dilution with D_2O to yield 250 μM HAPI ($[DMSO]_{final}$ = 2.5%). To obtain the HAPI* spectrum, the sample was partially submerged in a 4 °C ice bath and irradiated in a photoreactor for 10 min. The ice bath was replenished halfway through irradiation. Spectra were collected at 10 °C (Supporting Information Figure S4).

(Z)-HAPI (i.e., HAPI).* ^{1}H NMR (500 MHz, D_2O + 2.5% d_6-DMSO): δ ppm 8.38 (d, J = 5.36 Hz, 2H), 7.45 (d, J = 5.22 Hz, 2H), 7.13 (d, J = 7.84 Hz, 1H), 7.05 (dd, J = 7.65, 7.65 Hz, 1H), 6.57 (d, J = 8.13 Hz, 1H), 6.45 (dd, J = 7.46, 7.46 Hz, 1H), 2.18 (s, 1H).

(E)-HAPI. ^{1}H NMR (500 MHz, D_2O + 2.5% d_6-DMSO): δ ppm 8.35 (d, J = 5.54 Hz, 2H), 7.64 (d, J = 6.00 Hz, 2H), 7.40 (d, J = 8.00 Hz, 1H), 7.09 (dd, J = 7.43, 7.43 Hz, 1H), 6.58 (d, J = 8.29 Hz, 1H), 6.51 (dd, J = 7.6 Hz, 1 H), 2.43 (s, 3H).

Absorption Spectroscopy. UV−vis absorption spectra were collected on a Cary 50 UV/vis spectrophotometer using quartz cuvettes with 1-cm path length. For experiments tracking HAPI spectral changes, chelator concentration was 50 μM. The conversion of HAPI to HAPI* was monitored by collecting absorption spectra after 30 s intervals of irradiation.

The thermal relaxation from *Z* back to *E* was also observed spectroscopically. The absorption spectrum for HAPI was collected before and after a 5-min irradiation with UVA light. The solution was subsequently maintained in the dark, and spectra were collected every 60 min over the course of 12 h.

To determine the room-temperature half-life of HAPI*, a series of absorption spectra of freshly irradiated HAPI* were collected over 12 h. The absorbance data were converted to concentration by using extinction coefficients that were determined by knowing the relative concentration of each isomer in a nonirradiated solution and a fully irradiated (photostationary) solution from the chromatography data (HAPI, ε_{400} 4960 mol^{-1} cm^{-1}; HAPI*, ε_{400} = 270 mol^{-1} cm^{-1}, both at pH 7.4) The half-life was calculated from the exponential decay fit of the [(*Z*)-HAPI] versus time data.

To test for photoswitching properties, HAPI solutions were first irradiated with 350 nm-centered light (UVA). After a HAPI* absorption spectrum was collected, the solution was moved to another

dx.doi.org/10.1021/ic402221x | Inorg. Chem. 2014, 53, 1397−1405

photoreactor outfitted with RPR-2537 lamps (UVC). The solution was irradiated for 1 min prior to spectrum acquisition.

Metal Binding Studies. Stock solutions of the following metal salts were prepared at 1 and 100 mM concentrations in deionized water: $MgCl_2$, KCl, $CaCl_2$, $CrCl_3$, $MnCl_2$, $CoCl_2$, $NiCl_2$, $ZnCl_2$, $AlCl_3$, $(NH_4)_2Fe(SO_4)_2$, and $CuSO_4$ (or $CuCl_2$). The ferrous ammonium sulfate used as the iron source for all experiments was prepared fresh daily. Because the reactions are done in aerated aqueous solution, the iron complexes formed are oxidized to the ferric state.[59] Solutions containing equimolar quantities of HAPI and the respective metals were prepared in HEPES buffer (pH 7.5) at either at 50 or 10 μM concentrations depending on the subsequent complex solubility. Solutions were monitored spectrophotemetrically over 1 h to ensure sufficient time for complex formation. Solutions were irradiated for 5 min with UVA light, and then absorption spectra were recollected (Supporting Information Figure S5). For solutions showing light-induced spectral changes, new solutions containing 1:10 HAPI:M^{n+} were prepared. Several of these mixtures resulted in precipitation and were not further analyzed. For 1:10 solutions showing good solubility, a 5-min UVA irradiation was administered, and the absorption spectra were recollected. This process was repeated with 100 equiv of metal ion for those solutions that displayed photoreactivity.

Conditional Metal Binding Constants. The conditional binding affinities of HAPI for Cu^{2+}, Zn^{2+}, and Fe^{3+} were determined by competitive equilibrium titrations with metal-binding indicators of known affinity. The titrations were monitored spectrophotometrically, and the acquired spectra (from λ = 300 nm to λ = 800 nm) were analyzed with SPECFIT/32 Version 3.0.35 global analysis fitting software.[85] Reference spectra for the free indicator, the metal−indicator complex, and free HAPI were used to aid the data fitting by providing wavelength-dependent absorptivity values for the absorbing species in solution. The competition experiments were conducted in PBS or HEPES buffer at pH 7.4; therefore, the reported values represent the conditional binding affinity specifically under these conditions of buffer and pH.

Copper. The indicator PAR (4-(2-pyridylazo)resorcinol) forms a colored 1:1 complex with Cu^{2+} with a conditional binding constant at pH 7.4 (phosphate buffer) of 2.6×10^{-15}.[86,87] A working solution of PAR was prepared in PBS buffer, and its concentration was determined by using the extinction coefficient reported by Crow et al.[86] and further verified by titration with standardized $CuSO_4$. Aliquots of HAPI were titrated in 1 μL volumes from a 1 mM DMSO stock into 1 mL of a PBS solution containing 10 μM PAR and 10 μM $CuSO_4$. The solution was allowed to equilibrate for 5 min prior to spectrum acquisition after each addition, until no further spectral changes were observed. A 1:1 Cu:HAPI binding ratio was the only model that fit the competition data. This 1:1 model is consistent with known structures of other members of this hydrazone family coordinated to Cu^{2+},[69,71,88] and is also consistent with results of a direct titration of HAPI with Cu^{2+}, where the characteristic absorption bands of Cu−HAPI increase up to 1 equiv of added Cu. Excess Cu results in precipitation, which prohibits a full analysis by the method of continuous variation (data not shown). Using the PAR competition data, a conditional binding constant of HAPI for Cu^{2+} at pH 7.4 in PBS was calculated as log K'_{CuHAPI} of 14.7 ± 0.1.

Zinc. HAPI affinity for Zn^{2+} at pH 7.4 was determined by competition with 2-carboxy-2′-hydroxy-5′-sulfoformazyl-benzene (Zincon), a colorimetric ligand that binds Zn^{2+} in a 1:1 stoichiometry.[89] Portions of HAPI were titrated from a DMSO stock in 2-μL aliquots into a solution of 10 μM $ZnSO_4$ with 40 μM Zincon in 10 mM HEPES buffer (pH 7.4 + 100 mM NaCl) (Supporting Information Figure S8). The decrease in absorbance at 620 nm indicates removal of Zn^{2+} from the Zincon complex. Given a conditional binding constant for Zincon at pH 7.4 of log $K'_{Zn(Zincon)}$= 3.56,[89] the 1:1 Zn:HAPI model calculated log $K'_{Zn(HAPI)}$ = 3.6 ± 0.1.

Iron. A binding constant of HAPI for Fe^{3+} was found by competition with ethylenediaminetetraacetic acid (EDTA) (log $K'_{Fe(EDTA)}$ = 16.58 at pH 7.4, μ = 0.1 M; this value was calculated from the published β and acid dissociation constants).[90] Experiments were performed by generating a series of separate solutions in 10 mM HEPES (pH 7.4 + 100 mM NaCl) containing 300 μM HAPI, $[Fe]_{total}$ = 60 μM, and varying [EDTA] from 0 to 200 μM (Supporting Information Figure S8). The HAPI/EDTA competition was also performed in the reverse direction by altering [HAPI] from 0 to 400 μM in the presence of 20 μM Fe + 20 μM EDTA. The proportion of DMSO was held constant at 10% for all solutions, and the Fe source was standardized, aqueous ferrous ammonium sulfate. Solutions were mixed and then allowed to equilibrate in the dark overnight prior to acquiring spectra. During this time, ferrous ions complexed by either HAPI or EDTA oxidize to the +3 state.[59] For solutions above 150 μM HAPI, precipitation was observed, and these spectra were excluded from the SPECFIT data fitting. The model that best fit the data invokes a 1:2 metal:ligand ratio, as predicted on the basis of previous studies of aroylhydrazone iron chelators under similar conditions.[58] Consistent with this prediction, spectra of HAPI with increasing concentrations of iron show a linear increase in complex formation that plateaus at a 2:1 ratio, substantiating the presence of the $[Fe(HAPI)_2]^+$ complex under these conditions (Supporting Information Figure S7). The fitting results from titration in both directions agreed, resulting in a conditional binding constant for $[Fe(HAPI)_2]^+$ of log K' = 20.5 ± 0.2 in 10 mM HEPES (pH 7.4 + 100 mM NaCl).

Relative Binding Affinity of HAPI* As Compared to HAPI. Relative binding strengths of HAPI and HAPI* for Cu^{2+} were assessed by competition with 4-(2-pyridylazo)resorcinol (Figure 6). Aliquots of a stock solution of HAPI (1 mM in 9:1 HEPES: DMSO) were titrated into a solution containing 5 μM equimolar PAR and $CuSO_4$ in 10 mM HEPES buffer (pH 7.4 + 200 mM NaCl). The solution was equilibrated 5 min between additions, when no further spectral changes were observed. The absorption band at 510 nm was used to determine the concentration of Cu(PAR) after each addition, as no other species have appreciable absorption at this wavelength.

For the titration of Cu(PAR) with HAPI*, a 100 μM working solution of HAPI in HEPES buffer was irradiated for 5 min with UVA light in a photoreactor. Next, 5 μM $CuSO_4$, 5 μM PAR, and 1−5 equiv of freshly irradiated HAPI* were mixed in HEPES, and an absorption spectrum was collected immediately.

Relative binding strength of HAPI, HAPI*, and UVC-reconstituted HAPI (rHAPI) for Fe^{3+} (Figures 7 and Supporting Information Figure S10) was assessed by a calcein assay. The fluorescent probe calcein binds Fe^{2+} or Fe^{3+} to form 1:1 Fe:calcein complexes, which readily oxidize to the Fe^{3+} state in aerobic environments.[59,91] The fluorescence emission of calcein is quenched when coordinated to iron. Experiments were performed at 25 °C using black-walled 96-well plates with clear bottoms in a Wallac Victor 1420 plate reader equipped with F485 and F535 incident and emission filters, respectively. Stocks of HAPI, HAPI*, rHAPI, and Fe(calcein) were prepared immediately before use at 100 μM concentrations in HEPES buffer (pH 7.4 + 200 mM NaCl). HAPI* was generated by irradiating a 100 μM working HAPI solution with UVA light for 2 min. rHAPI was generated by first irradiating a 100 μM working HAPI solution with 2 min of UVA light, then irradiating the same solution with UVC lamps for 30 s. The Fe(calcein) stock solution was prepared by equilibrating equimolar $(NH_4)_2Fe(SO_4)_2$ and calcein (from a 1 mM stock in 1 M $NaHCO_3$) in HEPES buffer for 1 h to ensure formation of the ferric calcein complex. In each well, Fe(calcein) at a final concentration of 2 μM was combined with varying [HAPI], [HAPI*], or [rHAPI] in HEPES buffer. Emission values from triplicate wells were averaged for each condition. Wells containing only Fe(calcein) were used to determine 0% unquenching, while those containing Fe(calcein) + 25 equiv HAPI provided the 100% unquenching upper limit. These values were used in the following equation to calculate % dequenched calcein for each condition: % dequenching = $(E_i - E_{Fe})/(E_{25} - E_{Fe})$*100, where E_i is the average of three wells for an experimental condition, E_{Fe} is the average emission without added HAPI, and E_{25} is the emission for Fe(calcein) + 25 equiv HAPI.

Assessment of $[Fe(HAPI)_2]^+$ Photoreactivity. Iron-induced quenching of calcein fluorescence was used to detect any release of iron from irradiated solutions of the $[Fe(HAPI)_2]^+$ complex (Supporting Information Figure S9). A 100 μM stock solution of the $[Fe(HAPI)_2]^+$ was prepared by equilibrating $(NH_4)_2Fe(SO_4)_2$ and HAPI in HEPES

dx.doi.org/10.1021/ic402221x | Inorg. Chem. 2014, 53, 1397−1405

buffer in a 1:2 molar ratio at room temperature for 1 h to form the ferric complex. This stock solution was diluted into 2 mL of HEPES buffer in a quartz cuvette to prepare a 500 nM $[Fe(HAPI)_2]^+$ solution that was irradiated for 2 min in a photoreactor with UVA light. To the irradiated solution was added a 10-μL aliquot of 100 μM calcein, which was mixed thoroughly and equilibrated for 15 min in the dark prior to collecting fluorescence emission spectra on a Fluorolog-2 fluorometer (λ_{exc} = 487 nm).

■ ASSOCIATED CONTENT

Ⓢ Supporting Information

Computer modeling experimental details as well as LC/MS, ^{1}H NMR, and assorted UV/vis absorbance spectroscopy data. This material is available free of charge via the Internet at http://pubs.acs.org.

■ AUTHOR INFORMATION

Corresponding Author

*E-mail: katherine.franz@duke.edu.

Notes

The authors declare no competing financial interest.

■ ACKNOWLEDGMENTS

We thank the National Science Foundation for supporting this work (CHE-1552054 (K.J.F.) and CHE-09-11119 (W.Y.)). We thank Dr. George Dubay for assistance with LC/MS data collection. A.T.F. appreciates a Burroughs Wellcome Fellowship, and D.P. appreciates William Krigbaum and Marcus Hobbs Fellowships from the Department of Chemistry, Duke University.

■ REFERENCES

(1) Hartley, G. S. *Nature* **1937**, *140*, 281.
(2) Hartley, G. S. *J. Chem. Soc.* **1938**, 633.
(3) Bandara, H. M. D.; Burdette, S. C. *Chem. Soc. Rev.* **2012**, *41*, 1809.
(4) Beharry, A. A.; Sadovski, O.; Wong, L.; Tropepe, V.; Woolley, G. A. *Biopolymers* **2011**, *96*, 431.
(5) Beharry, A. A.; Sadovski, O.; Woolley, G. A. *J. Am. Chem. Soc.* **2011**, *133*, 19684.
(6) Garcia-Amoros, J.; Diaz-Lobo, M.; Nonell, S.; Velasco, D. *Angew. Chem., Int. Ed.* **2012**, *51*, 12820.
(7) Haberhauer, G.; Kallweit, C. *Angew. Chem., Int. Ed.* **2010**, *49*, 2418.
(8) Hashim, P. K.; Thomas, R.; Tamaoki, N. *Chem.—Eur. J.* **2011**, *17*, 7304.
(9) Yu, G.; Han, C.; Zhang, Z.; Chen, J.; Yan, X.; Zheng, B.; Liu, S.; Huang, F. *J. Am. Chem. Soc.* **2012**, *134*, 8711.
(10) Berryman, O. B.; Dube, H.; Rebek, J. *Isr. J. Chem.* **2011**, *51*, 700.
(11) Deloncle, R.; Caminade, A. M. *J. Photochem. Photobiol., C* **2010**, *11*, 25.
(12) Feng, W.; Luo, W.; Feng, Y. Y. *Nanoscale* **2012**, *4*, 6118.
(13) Merino, E.; Ribagorda, M. *Beilstein J. Org. Chem.* **2012**, *8*, 1071.
(14) Natali, M.; Giordani, S. *Chem. Soc. Rev.* **2012**, *41*, 4010.
(15) Russew, M.-M.; Hecht, S. *Adv. Mater.* **2010**, *22*, 3348.
(16) Bouas-Laurent, H.; Durr, H. *Pure Appl. Chem.* **2001**, *73*, 639.
(17) Szymański, W.; Beierle, J. M.; Kistemaker, H. A. V.; Velema, W. A.; Feringa, B. L. *Chem. Rev.* **2013**.
(18) Bruder, F. K.; Hagen, R.; Rolle, T.; Weiser, M. S.; Facke, T. *Angew. Chem., Int. Ed.* **2011**, *50*, 4552.
(19) Yu, H. F.; Ikeda, T. *Adv. Mater.* **2011**, *23*, 2149.
(20) Al-Atar, U.; Fernandes, R.; Johnsen, B.; Baillie, D.; Branda, N. R. *J. Am. Chem. Soc.* **2009**, *131*, 15966.
(21) Liu, D.; Xie, Y.; Shao, H.; Jiang, X. *Angew. Chem., Int. Ed.* **2009**, *48*, 4406.
(22) Fortin, D. L.; Banghart, M. R.; Dunn, T. W.; Borges, K.; Wagenaar, D. A.; Gaudry, Q.; Karakossian, M. H.; Otis, T. S.; Kristan, W. B.; Trauner, D.; Kramer, R. H. *Nat. Methods* **2008**, *5*, 331.
(23) Banghart, M.; Borges, K.; Isacoff, E.; Trauner, D.; Kramer, R. H. *Nat. Neurosci.* **2004**, *7*, 1381.
(24) Gorostiza, P.; Volgraf, M.; Numano, R.; Szobota, S.; Trauner, D.; Isacoff, E. Y. *Proc. Natl. Acad. Sci. U.S.A.* **2007**, *104*, 10865.
(25) Shimomura, M.; Kunitake, T. *J. Am. Chem. Soc.* **1982**, *104*, 1757.
(26) Volgraf, M.; Gorostiza, P.; Numano, R.; Kramer, R. H.; Isacoff, E. Y.; Trauner, D. *Nat. Chem. Biol.* **2006**, *2*, 47.
(27) Balzani, V.; Credi, A.; Marchioni, F.; Stoddart, J. F. *Chem. Commun.* **2001**, 1860.
(28) Balzani, V.; Credi, A.; Venturi, M. *Chem. Soc. Rev.* **2009**, *38*, 1542.
(29) Kimura, K.; Sakamoto, H.; Nakamura, M. *Bull. Chem. Soc. Jpn.* **2003**, *76*, 225.
(30) Minkin, V. I. *Russ. Chem. Rev.* **2013**, *82*, 1.
(31) Shinkai, S.; Nakaji, T.; Ogawa, T.; Shigematsu, K.; Manabe, O. *J. Am. Chem. Soc.* **1981**, *103*, 111.
(32) Shinkai, S.; Shigematsu, K.; Sato, M.; Manabe, O. *J. Chem. Soc., Perkin Trans. 1* **1982**, 2735.
(33) Collins, G. E.; Choi, L.-S.; Ewing, K. J.; Michelet, V.; Bowen, C. M.; Winkler, J. D. *Chem. Commun.* **1999**, 321.
(34) Phillips, J. P.; Mueller, A.; Przystal, F. *J. Am. Chem. Soc.* **1965**, *87*, 4020.
(35) Kimura, K.; Kaneshige, M.; Yamashita, T.; Yokoyama, M. *J. Org. Chem.* **1994**, *59*, 1251.
(36) Preigh, M. J.; Lin, F.-T.; Ismail, K. Z.; Weber, S. G. *J. Chem. Soc., Chem. Commun.* **1995**, 2091.
(37) Collins, G. E.; Choi, L. S.; Ewing, K. J.; Michelet, V.; Bowen, C. M.; Winkler, J. D. *Chem. Commun.* **1999**, 321.
(38) Chaur, M. N.; Collado, D.; Lehn, J.-M. *Chem.—Eur. J.* **2011**, *17*, 248.
(39) Padwa, A. *Chem. Rev.* **1977**, *77*, 37.
(40) Vantomme, G.; Lehn, J.-M. *Angew. Chem., Int. Ed.* **2013**, *52*, 3940.
(41) Araujo-Andrade, C.; Giuliano, B. M.; Gómez-Zavaglia, A.; Fausto, R. *Spectrochim. Acta, Part A* **2012**, *97*, 830.
(42) Pratt, A. C. *Chem. Soc. Rev.* **1977**, *6*, 63.
(43) *The Chemistry of the Carbon-Nitrogen Double Bond*; Patai, S., Ed.; Interscience Publishers: New York, 1970.
(44) Becker, R. S.; Chagneau, F. *J. Am. Chem. Soc.* **1992**, *114*, 1373.
(45) Kovarikova, P.; Vavrova, K.; Tomalova, K.; Schongut, M.; Hruskova, K.; Haskova, P.; Klimes, J. *J. Pharm. Biomed. Anal.* **2008**, *48*, 295.
(46) Zhao, L. Y.; Sui, D.; Chai, J.; Wang, Y.; Jiang, S. M. *J. Phys. Chem. B* **2006**, *110*, 24299.
(47) Becker, R. S.; Richey, W. F. *J. Am. Chem. Soc.* **1967**, *89*, 1298.
(48) Su, X.; Aprahamian, I. *Org. Lett.* **2011**, *13*, 30.
(49) Cao, X.; Zeng, X.; Mu, L.; Chen, Y.; Wang, R.-x.; Zhang, Y.-q.; Zhang, J.-x.; Wei, G. *Sens. Actuators, B* **2013**, *177*, 493.
(50) Condorelli, G.; Costanzo, L. L.; Alicata, L.; Giuffrida, A. *Chem. Lett.* **1975**, 227.
(51) Costanzo, L. L.; Chiacchio, U.; Giuffrida, S. *J. Photochem.* **1980**, *13*, 83.
(52) Costanzo, L. L.; Giuffrida, S.; Chiacchio, U.; Condorelli, G. *J. Photochem.* **1979**, *11*, 39.
(53) Pichon, R.; Lesaint, J.; Courtot, P. *Tetrahedron* **1981**, *37*, 1517.
(54) Landge, S. M.; Aprahamian, I. *J. Am. Chem. Soc.* **2009**, *131*, 18269.
(55) Landge, S. M.; Tkatchouk, E.; Benitez, D.; Lanfranchi, D. A.; Elhabiri, M.; Goddard, W. A.; Aprahamian, I. *J. Am. Chem. Soc.* **2011**, *133*, 9812.
(56) Ray, D.; Foy, J. T.; Hughes, R. P.; Aprahamian, I. *Nat. Chem.* **2012**, *4*, 757.
(57) Su, X.; Robbins, T. F.; Aprahamian, I. *Angew. Chem., Int. Ed.* **2011**, *50*, 1841.
(58) Ponka, P.; Borova, J.; Neuwirt, J.; Fuchs, O. *FEBS Lett.* **1979**, *97*, 317.

(59) Hruskova, K.; Kovarikova, P.; Bendova, P.; Haskova, P.; Mackova, E.; Stariat, J.; Vavrova, A.; Vavrova, K.; Simunek, T. *Chem. Res. Toxicol.* **2011**, *24*, 290.
(60) Bernhardt, P. V.; Wilson, G. J.; Sharpe, P. C.; Kalinowski, D. S.; Richardson, D. R. *J. Biol. Inorg. Chem.* **2008**, *13*, 107.
(61) Kovarikova, P.; Mrkvickova, Z.; Klimes, J. *J. Pharm. Biomed. Anal.* **2008**, *47*, 360.
(62) Kalinowski, D. S.; Sharpe, P. C.; Bernhardt, P. V.; Richardson, D. R. *J. Med. Chem.* **2008**, *51*, 331.
(63) Kovacevic, Z.; Kalinowski, D. S.; Lovejoy, D. B.; Yu, Y.; Rahmanto, Y. S.; Sharpe, P. C.; Bernhardt, P. V.; Richardson, D. R. *Curr. Top. Med. Chem.* **2011**, *11*, 483.
(64) Bendova, P.; Mackova, E.; Haskova, P.; Vavrova, A.; Jirkovsky, E.; Sterba, M.; Popelova, O.; Kalinowski, D. S.; Kovarikova, P.; Vavrova, K.; Richardson, D. R.; Simunek, T. *Chem. Res. Toxicol.* **2010**, *23*, 1105.
(65) Richardson, D.; Vitolo, L. W.; Bakers, E.; Webb, J. *Biol. Met.* **1989**, *2*, 69.
(66) Charkoudian, L. K.; Pham, D. M.; Kwon, A. M.; Vangeloff, A. D.; Franz, K. J. *Dalton Trans.* **2007**, 5031.
(67) Roy, S.; Mandal, T. N.; Barik, A. K.; Gupta, S.; Fallah, M. S. E.; Tercero, J.; Butcher, R. J.; Kar, S. K. *Dalton Trans.* **2009**, 8215.
(68) Li, L.; Zhu, L.; Chen, D.; Hu, X.; Wang, R. *Eur. J. Org. Chem.* **2011**, *2011*, 2692.
(69) Wu, L. M.; Teng, H. B.; Ke, X. B.; Xu, W. J.; Su, J. T.; Liang, S. C.; Hu, X. M. *Chem. Biodiversity* **2007**, *4*, 2198.
(70) Aruffo, A. A.; Murphy, T. B.; Johnson, D. K.; Rose, N. J.; Schomaker, V. *Inorg. Chim. Acta* **1982**, *67*, L25.
(71) Aruffo, A. A.; Murphy, T. B.; Johnson, D. K.; Rose, N. J.; Schomaker, V. *Acta Crystallogr., Sect. C: Cryst. Struct. Commun.* **1984**, *40*, 1164.
(72) Matoga, D.; Szklarzewicz, J.; Stadnicka, K.; Shongwe, M. S. *Inorg. Chem.* **2007**, *46*, 9042.
(73) Murphy, T. B.; Rose, N. J.; Schomaker, V.; Aruffo, A. *Inorg. Chim. Acta* **1985**, *108*, 183.
(74) Becke, A. D. *J. Chem. Phys.* **1993**, *98*, 5648.
(75) Lee, C. T.; Yang, W. T.; Parr, R. G. *Phys. Rev. B* **1988**, *37*, 785.
(76) Frisch, M. J.; et al. *Gaussian 09*; Gaussian Inc.: Wallingford, CT, 2009. Full citation in the Supporting Information.
(77) Zhao, Y.; Truhlar, D. G. *J. Phys. Chem. A* **2005**, *109*, 5656.
(78) Richardson, D.; Ponka, P. *J. Lab. Clin. Med.* **1998**, *131*, 306.
(79) Singh, R.; Jain, P.; Singh, R. *Talanta* **1982**, *29*, 77.
(80) Platte, J.; Marcy, V. *Anal. Chem.* **1959**, *31*, 1226.
(81) Sastry, P. S. J.; Rao, T. R. *Proc.-Indian Acad. Sci., Chem. Sci.* **1995**, *107*, 25.
(82) Rush, R. M.; Yoe, J. H. *Anal. Chem.* **1954**, *26*, 1345.
(83) Sakiyama, H.; Mochizuki, R.; Sugawara, A.; Sakamoto, M.; Nishida, Y.; Yamasaki, M. *Dalton Trans.* **1999**, 997.
(84) Kielar, F.; Helsel, M. E.; Wang, Q.; Franz, K. J. *Metallomics* **2012**, *4*, 899.
(85) Binstead, R. A. Z.; Jung, B. *SPECFIT/32 Version 3.0.35*; 2004.
(86) Crow, J. P.; Sampson, J. B.; Zhuang, Y. X.; Thompson, J. A.; Beckman, J. S. *J. Neurochem.* **1997**, *69*, 1936.
(87) Iwamoto, T. *Bull. Chem. Soc. Jpn.* **1961**, *34*, 605.
(88) Johnson, D. K.; Murphy, T. B.; Rose, N. J.; Goodwin, W. H.; Pickart, L. *Inorg. Chim. Acta* **1982**, *67*, 159.
(89) Shaw, C. F.; Laib, J. E.; Savas, M. M.; Petering, D. H. *Inorg. Chem.* **1990**, *29*, 403.
(90) Motekaitis, R. J. *NIST Standard Reference Database 46: NIST Critically Selected Stability Constants of Metal Complexes*, 6.0 ed.; Martell, A. E. S., Ed.; NIST: Gaithersburg, MD, 2001.
(91) Breuer, W.; Epsztejn, S.; Cabantchik, Z. I. *J. Biol. Chem.* **1995**, *270*, 24209.